



Molecular characterisation and structural assessment of an RXLR effector from *Phytophthora palmivora*, the coconut bud rot pathogen

K.P. Gangaraj^{1,2} and M.K. Rajesh^{1,*}

¹ICAR-Central Plantation Crops Research Institute, Kasaragod- 671124, Kerala, India

² Mangalore University, Mangalagangothri, Mangaluru-574199, Karnataka, India

(Manuscript Received: 18-05-2020, Revised: 04-09-2020, Accepted: 15-04-2022)

Abstract

Phytophthora species are phytopathogenic oomycetes that damage a wide variety of crops. *Phytophthora* delivers effectors, which are secretory proteins, into the host cells. Effectors promote infection by reprogramming the host cellular machinery and are key determinants of oomycete virulence. The major class of *Phytophthora* effector proteins contains the RXLR motif. In this study, we have carried out the molecular and structural characterisation of an RXLR effector (RXLR6744) from a virulent *P. palmivora* isolated from bud rot disease-affected coconut palm. The open reading frame (ORF) of the RXLR6744, amplified using RT-PCR, had a length of 411 bp. The gene was found to encode a predicted protein of 136 amino acids and had a molecular weight of 15.52 kDa. Phylogenetic analysis of the amino acid sequence revealed that it was closely related to RXLR proteins from *P. palmivora* (causing black pod disease in cocoa) and related species *P. megakarya*. Topology analysis revealed that the protein was composed of six α -helices. The structural prediction was undertaken by computer-aided homology modelling. From the Ramachandran plot analysis, it could be observed that the majority (96.3%) of amino acids were present in the preferred region, 3.7 per cent of amino acid residues were present in the allowed region, and no residues were observed in the disallowed region. The structure showed an average quality of 94.4 per cent, indicating it to be a high-quality structure. This study provides the detailed characterisation of an RXLR effector from *P. palmivora*. It will aid the elucidation of its role in pathogenesis and facilitate further refined investigations of the structure/function relationships of oomycete effectors.

Keywords: Effectors, homology modelling, *Phytophthora palmivora*, RXLR

Introduction

Plant diseases are a significant yield and quality constraint for plantation crops. Phytopathogens can be fungal, bacterial, viral or phytoplasma and can damage plant parts above or below the ground. Among phytopathogenic oomycetes, *Phytophthora* is a major genus responsible for impairment for economically important crops worldwide and inflicting serious damage to natural ecosystems (Erwin *et al.*, 1996). More than 200 species of *Phytophthora* have been identified; prominent members include *P. infestans*, *P. sojae*, *P. ramorum* and *P. cinnamomi* (Riolo *et al.*, 2020; Scanu *et al.*, 2021). The Great Irish Famine, which occurred due

to late blight disease in potatoes caused by *P. infestans*, resulted in the loss of millions of lives in Ireland from 1845 to 1852 (Yoshida *et al.*, 2013). A tropical relative of *P. infestans*, with its origins in south-eastern Asia, is *Phytophthora palmivora* (McHau and Coffey, 1994), with international trade aiding in its spread world over (Scott, 2013).

The host range of *P. palmivora* is wide, and virulence has been established in the roots and leaves of both monocotyledons and dicotyledons (Rey *et al.*, 2015). It causes root/bud/fruit rot diseases in many important tropical fruits, spices and oil seeds (Drenth and Sendall, 2004). As a hemibiotroph, *P. palmivora* first parasitises living

*Corresponding Author: rajesh.mk@icar.gov.in

tissues; it grows and sporulates in dead tissues. Motile zoospores infect plants when they come into contact with plant surfaces; they encyst, germinate and form appressoria, which aid penetration of the plant surface (Judelson and Blanco, 2005). Once the pathogen has gained access to plant tissues, it develops ‘digit-like’ haustoria that protrude into living plant cells and release virulent effector proteins that cause the plant to be infected. A necrotrophic stage follows, characterised by necrosis of host tissue and the release of zoospores from sporangia (Zuluaga *et al.*, 2016).

Phytophthora spp. secrete many effector proteins, and these proteins have specific sites of action. Apoplastic effectors enter the extracellular spaces of plants, while cytoplasmic effectors are translocated into the plant’s cells and target sub-cellular regions (Birch *et al.*, 2006; Kamoun, 2006; Hunziker *et al.*, 2021). By inhibiting host proteases and glucanases, which accumulate in response to pathogen infection, apoplastic effectors contribute to counter-defence (Rose *et al.*, 2002; Tian *et al.*, 2004, 2005). Contrary to this, cytoplasmic effectors are poorly understood in terms of their biochemical activities. The RXLR family of *Phytophthora* cytoplasmic effectors was discovered through their avirulence (*Avr*) function, *i.e.*, their ability to trigger hypersensitive cell death on genotypes with corresponding disease resistance genes (*R*) (Armstrong *et al.*, 2005; Rehmany *et al.*, 2005; Chepsergon *et al.*, 2021).

As the infection progresses through the biotrophic phase, phytophthoral cytoplasmic effectors play a crucial role in virulence. An RXLR effector consists of a secretion signal peptide followed by a conserved N-terminal domain with the RXLR consensus sequence (Arg-Xaa-Leu-Arg). The translocation of these effectors inside plant cells depends on the RXLR domain (Whisson *et al.*, 2007). C-terminal regions of these effectors appear to be involved in their biochemical activity (Schornack *et al.*, 2009). The N-terminal part of *Avr1b* contains a signal peptide (SP) and the RXLR-dEER domain, which contains the RXLR motif and the dEER motif. RXLR proteins display a high degree of sequence diversity in their effector domains. However, it is important to note that despite this diversity, there are some recognisable sequence relationships within the C-terminal regions

of RXLR effectors and some repeating sequence motifs such as ‘W’, ‘Y’, and ‘L’ (Jiang, 2008). Nearly half of RXLR effectors possess the W, Y, and L motifs. In contrast to the RXLR motif, the ‘dEER’ motif has a stretch of primarily acidic amino acids (Shan *et al.*, 2004; Kamoun, 2006; van Poppel *et al.*, 2008).

Despite the economic impact and widespread distribution of *P. palmivora* in coconut and other palms, no studies have been undertaken on the characterisation of the effector protein repertoire of *P. palmivora*. In the present study, we have amplified the full-length coding sequence of a highly expressed RXLR (*RXL6744*), identified from our previous coconut-*P. palmivora* interaction studies undertaken using dual RNA-sequencing (dual RNA-seq) (Gangaraj and Rajesh, 2020). We have also predicted the three-dimensional structure (3-D) of the RXLR protein. The findings could help us understand how the RXLR proteins function as an effector to aid oomycete pathogenesis and establish target molecules to control *P. palmivora*.

Materials and methods

Primer designing

We have selected a highly expressed RXLR transcript (*RXL6744*), identified from dual RNA-seq data generated in-house (Gangaraj and Rajesh, 2020). Enhanced expression of this transcript was observed at 24 hours post inoculation (hpi) of pin-pricked coconut leaflets with the virulent *P. palmivora* TR-PP-2 isolate (Gangaraj *et al.*, 2021). The full-length coding sequence (cds) was picked up from the genome sequence of the *P. palmivora*, incitant of oil palm disease (isolate ZC01), which is available in NCBI (Genome ID: 66939; GenBank assembly accession: GCA_008079305.1; Sequence ID: VOQZ01000128.1: 107016-107426). The full-length RXLR gene was retrieved from NCBI-Genbank (Sequence ID: VOQZ01000128.1: 106805-107448) through BLAST analysis. Primer3 (v. 0.4.0) (<http://bioinfo.ut.ee/primer3-0.4.0/>) programme was utilised to design primers to amplify the full-length coding sequence of the RXLR effector.

In vitro inoculation assay and RNA isolation

This study used a previously isolated and characterised virulent strain of *P. palmivora*

(TR-PP-2) (Gangaraj and Rajesh, 2020; Gangaraj *et al.*, 2021). Using the *in vitro* inoculation assay developed (Gangaraj and Rajesh, 2020; Gangaraj *et al.*, 2021), seven-day-old culture disks of the TR-PP-2 isolate were inoculated onto *in vitro* maintained and pin-pricked coconut leaflets of Chowghat Orange Dwarf cultivar. Total RNA was extracted 24 h post-inoculation (hpi) utilising the NucleoSpin RNA Plant and Fungi kit (Macherey Nagel, Germany). The OD 260 nm/280 nm ratio was used to evaluate the RNA quality and purity. The RNA Integrity Number (RIN) was determined using an Agilent 2100 Bioanalyzer (Agilent Technologies) and was observed to be >8.0. The high-quality RNA was stored at -80 °C until it was used in the next step of the process.

RT-PCR analysis

RNA samples were reverse transcribed to generate first-strand complementary DNA (cDNA) using the PrimeScript™ 1st strand cDNA Synthesis Kit (DSS Takara). GRXLRM-forward (5'-GGGATA CTCGAGACGCCAAG-3') and GRXLRM reverse (5'-GAGGCGATAGAGCACCTCAC-3') primers were used for amplifying the full-length cds of the RT-PCR analysis. The RT-PCR reaction mix consisted of 0.3 µL of *Taq* polymerase (1U/µL); 2 µL of 10x *Taq* Buffer A (GeNei™), 0.8 µL of 10 mM dNTP mix (GeNei™), 0.2 µM each of forward and reverse primer (Eurofins Genomics) and 1 µL (~200 ng) of synthesised cDNA, in a total volume of 20 µL. The reaction conditions were initial denaturation at 95 °C for 5 minutes and then 94 °C for 35 seconds, 55 °C for 1 minute, 72 °C for 1 minute for about 35 cycles, and a final extension at 72 °C for about 10 minutes (MyCycler™ Thermal Cycler; Bio-Rad). The amplicon was cloned in a T/A cloning vector (pTZ57R/T; InsTAclone™ PCR Cloning Kit; Thermo Fisher Scientific). Colony PCR was carried out using GRXLRM-forward and GRXLRM-reverse primers. Plasmid DNAs from positive clones were extracted with plasmid purification kits (QIAprep Spin Miniprep Kit; Qiagen). The inserts were sequenced, in an ABI Prism 377 automated DNA sequencer, by Sanger's method.

Sequence analysis of RXLR effector

The sequence was processed using BioEdit 7.2 (<http://en.bio-soft.net/format/BioEdit.html>) and

CAP3 (<http://doua.prabi.fr/software/cap3>) programmes. The open reading frame (ORF) was predicted with ORF Finder (<https://www.ncbi.nlm.nih.gov/orffinder/>) and compared to other *Phytophthora* spp. using Basic Local Alignment Search Tool (BLAST) analysis in National Center for Biotechnology Information (NCBI, <http://www.ncbi.nlm.nih.gov/>). With 1,000 bootstrap replicates, phylogenetic relationships of protein sequence were inferred using the Neighbor-Joining (NJ) approach (MEGA X version 10.2.4; <https://www.megasoftware.net/>). ProtParam (<http://web.expasy.org/protparam/>) was used to compute the theoretical pI, molecular weight and amino acid composition. SignalP-5.0 (<http://www.cbs.dtu.dk/services/SignalP/>) was used to determine the presence of signal peptides and their cleavage sites based on the predicted amino acid sequence of the effector protein. TargetP 1.1 (<http://www.cbs.dtu.dk/services/TargetP-1.1/index.php>) was used to predict the subcellular location of eukaryotic proteins, and TMHMM-2.0 (<http://www.cbs.dtu.dk/services/TMHMM/>) were used to identify the transmembrane helices in proteins. The secondary structure information was predicted using Sopma (https://npsa-prabi.ibcp.fr/cgi-bin/npsa_automat.pl?page=/NPSA/npsa_sopma.html) and Jpred 4 (<http://www.compbio.dundee.ac.uk/jpred/>).

Three-dimensional structure prediction of RXLR protein

Prediction of the three-dimensional (3D) structure of the RXLR protein was made by using the fold recognition ('threading') method since homology-based modelling could not be performed due to the lack of template structures in the Protein Data Bank (PDB). Two different servers, *viz.*, Phyre2 (<http://www.sbg.bio.ic.ac.uk/~phyre2/html/page.cgi?id=index>) and SPARKS-X (<https://sparks-lab.org/server/sparks-x/>), were used to predict the 3D models. Ramachandran plot validation was done on the predicted structure by utilising the SAVES server (<https://saves.mbi.ucla.edu/>). ModRefiner (<https://zhanglab.ccmb.med.umich.edu/ModRefiner/>) was used for high-level refinement of the predicted structure. The refined model was further validated through the SAVES server and ProSA-web (<https://prosa.services.came.sbg.ac.at/prosa.php>). PDBsum server (<http://www.ebi.ac.uk/thornton-srv/databases/cgi-bin/pdbsum/>

GetPage.pl?pdbcode=index.html) was used to study the topology.

Results and discussion

Amplification of RXLR region

A sequence of 411 bp length was obtained using GRXLRM-forward and GRXLRM-reverse primers. A standalone BLAST sequence search against the *P. palmivora* (isolate) was performed and showed maximum similarity. The complete cds were translated, and 136 amino acid length RXLR effector was identified without any introns. The sequence was deposited in NCBI (Accession no. MW768152).

Primary sequence analysis

Sequence alignment analysis of the sequenced product indicated perfect identity with secreted RXLR effector sequences from *P. palmivora* available in the Genbank database. The BLAST analysis showed 99.26 per cent homology with the subject sequence (GenBank accession no: POM73696.1) (Supplementary File 1). According to phylogenetic analysis, RXLR protein (coconut bud rot) was genetically similar to RXLR protein from *P. palmivora* isolate (cocoa) (GenBank accession no. POM73696) and closely related to

RXLR protein (GenBank accession no: OWZ10115) from *P. megakarya* (Fig. 1); the detailed information is available in Supplementary File 2. The primary sequence analysis, using ProtParm, showed that the predicted molecular weight of RXLR protein was 15518.56 Da. The total number of negatively charged residues (*viz.*, Asp + Glu) and positively charged residues (*viz.*, Arg + Lys) was 16 and 20, respectively. The instability index (II) is computed as 29.52; this classified the protein as stable. An analysis of the atomic composition of the protein sequence revealed 675 carbon atoms, 1079 hydrogen atoms, 207 nitrogen atoms, 204 oxygen atoms and five sulphur atoms. The grand average of hydropathicity (GRAVY) was -0.623, which indicates hydrophilicity.

Characteristics of RXLR effector

The SignalP 5.0 server predicted the presence of signal peptides (1-25 amino acid regions) and the location of their cleavage sites (25 and 26) in the RXLR protein. The TargetP predicted protein analysis indicates the protein located in the 'secretory pathway', and the signal peptide found in the sequence showed the highest score (0.928). Transmembrane analysis was carried out through an HMM-based method using TMHMM; the analysis revealed that RXLR was an extracellular

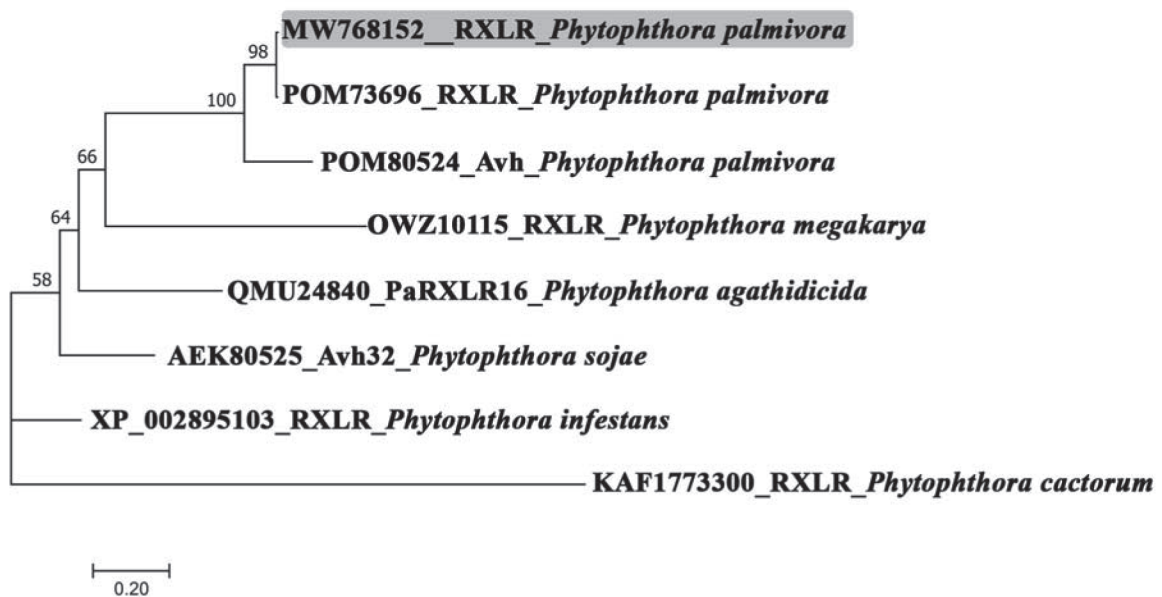


Fig. 1. Phylogenetic analysis of the protein sequence showed that the selected RXLR sequence was closely related to the RXLR protein sequence of *P. palmivora* and *P. megakarya*

protein. InterProScan explained that the protein was a modular protein comprising of a signal peptide domain (1-25), RXLR domain (47-51) and effector domain (62-136). The CDD analysis showed that the sequence contained the RXLR domain with a threshold of 1.66×10^{-13} . Sequence modules (W, Y, and L) were observed in the C-terminal domain of RXLR (Fig. 2).

The MEME predicted motifs in protein sequence showed the presence of RXLR and dEER motifs. The conserved RXLR motif (Arg-Xaa-Leu-Arg) is followed by a high proportion of acidic residues (D/E). Analysis of the secondary structure, using JPred 4, showed that the protein contains five helical regions (Fig. 2). The SOPMA secondary structure prediction indicated that the *P. palmivora* RXLR protein sequence contained 52.94 per cent (72) of alpha-helices (Hh), 6.62 per cent (9) of beta-turns (Tt), 9.56 per cent (13) of extended strands (Ee) and 30.88 per cent (42) of random coils (Cc).

Structural prediction of RXLR protein

SPARKS-X and Phyre 2 programmes were used to predict the 3D structure of RXLR *via* threading processes, and the Ramachandran plot was utilised to evaluate the overall quality of the structure. While the structure predicted by SPARKS-X contained more than 90 per cent residues in the favoured region, the structure predicted by Phyre 2 showed less than 80 per cent residues in the favoured

region. The predicted structure generated by SPARKS-X was therefore used for further study. SAVES analysed the Ramachandran plot of 'model.4.pdb' with 94.0 per cent amino acid residues in the favoured region, 4.5 per cent in the allowed region and just 1.5 per cent in the outer layer, respectively (Table 1). As approximately 94 per cent of the residues fall in the favoured region, the model was found to be good and reliable, and this model was selected for model refinement.

ModRefiner server has been used to reduce energy for the predicted structure's refinement. Once again, quality evaluation using SAVES was performed in the refinement model. The structure showed the highest percentage (96.3%) of amino acid in the favoured region, five (3.7%) amino acid residues in the allowed and no residue was observed in the disallowed region. The structure showed an overall quality of 94.4 per cent and was considered a high-quality structure. The ProSA score (Z-Score) of -4.02 for the model indicates that the energetic architecture of the predicted structure was good (Fig. 3). PDBsum server was used to study the topology of the refined structure. The findings revealed that the structure consisted of six alpha helices, eight helix-helix interactions, and three each of beta and gamma turns.

The structural topology revealed that the signal peptide was obtained in a single helical unit. The effector domain is composed of two alpha-helical units;

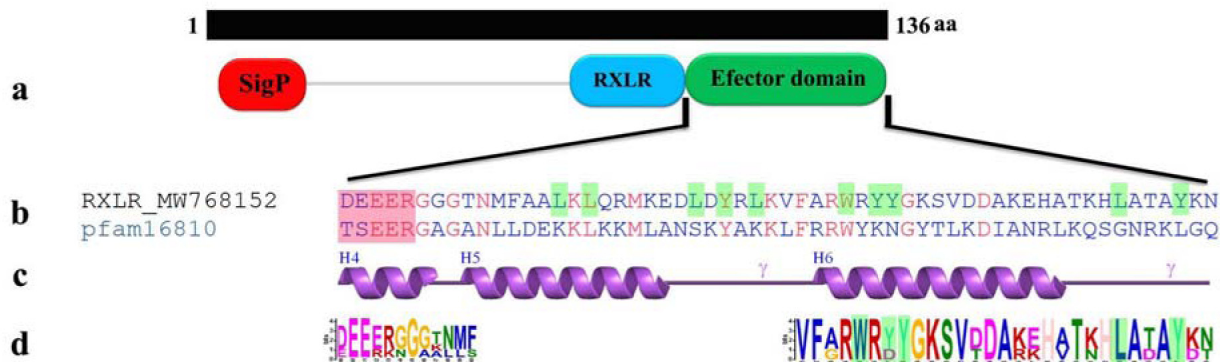


Fig. 2. Characteristics of RXLR protein. (a) Domain representation of RXLR protein. (b) Effector domain sequence analysis- the red boxes represent the dEER motif, and the green boxes represent the Tryptophan (W), Tyrosine (Y), and Leucine (L) positions. (c) Secondary structural elements of the effector domain. (d) MEME motif identification of effector domain; MEME sequence motifs define connected 'W-Y-L' modules

Table 1. Structural summary and Ramachandran plot validation details of predicted structures of RXLR using SPARKS-X server

Model	Z score	Structural details				Ramachandran plot validation		
		Group	Helices	Strands	Turns	Favoured region (%)	Allowed region (%)	Outlier region (%)
Model.1 .pdb	-2.82	136	8	0	12	91.8	4.5	3.7
Model.2 .pdb	-5.06	136	7	0	10	91.8	6.7	1.5
Model.3 .pdb	-3.8	136	6	0	15	93.3	5.2	1.5
Model.4 .pdb	-3.05	136	6	0	8	94.0	4.5	1.5
Model.5 .pdb	-3.8	136	6	0	9	91.0	4.5	4.5
Model.6 .pdb	-3.84	136	5	2	16	90.3	4.5	5.2

the region is the major functional unit of the RXLR effector. The targeting region is mainly composed of four alpha helical units; this region contains RXLR and dEER motifs.

Plant pathogens secrete effectors, which enable host invasion by overcoming the plant immune responses (Petre *et al.*, 2020). *Phytophthora* spp. ubiquitously secrete RXLR proteins onto host cell surfaces or into host cells; these proteins play a significant and integral role in pathogenesis (Chepsergon *et al.*, 2021). Characterisation of RXLR effectors has been reported in *P. infestans* (Wang *et al.*, 2019), *P. parasitica* (Huang *et al.*,

2019) and *P. sojae* (Wang *et al.*, 2019). To resolve the effector structure characteristics of a highly expressed RXLR effector from *P. palmivora* incitant of coconut bud rot, we have sequenced the cds of RXLR (RXI6744) from *P. palmivora* and translated it into protein for structure prediction.

The sequenced product had a length of 411 bp, and a BLAST search revealed a perfect match with *P. palmivora* RXLR sequences. The translated RXLR was a 136 amino acid long effector, without any introns, as translated from the ORF Finder from NCBI. Wide variations have been reported in the size of the RXLR protein, with the length ranging

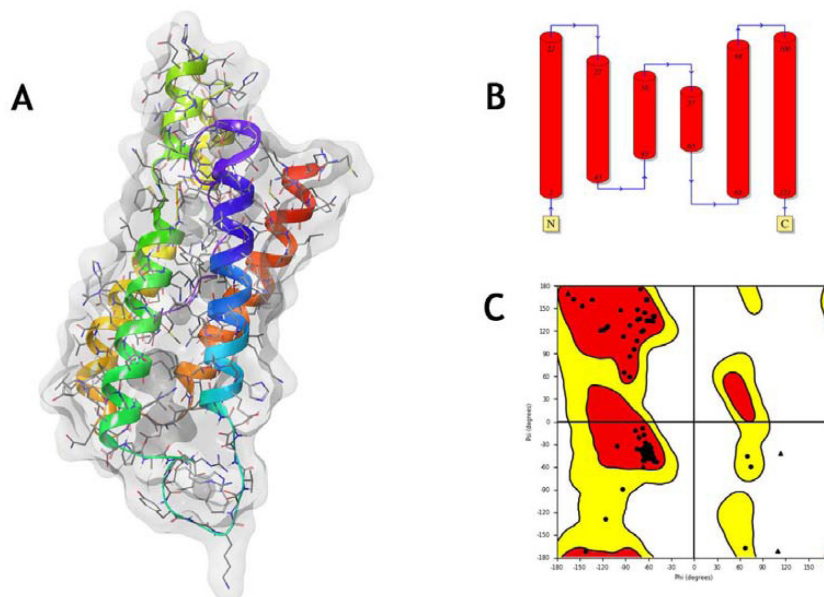


Fig. 3. Predicted 3D structure of RXLR effector. A. Predicted three-dimensional structure; B. Structural topology of the predicted model; C. Ramachandran plot validation of predicted model 4

from 84-381 amino acids (Petre *et al.*, 2020). The RXLR gene investigated here did not have introns, a feature shared by many oomycete RXLR effectors (Jiang *et al.*, 2008; Ai *et al.*, 2020). For the effectors of the RXLR family to be translocated into the plant cell, the RXLR motif appears to be essential; however, it is not essential for the biochemical activity of RXLR effectors (Zhao *et al.*, 2018).

The probed C-terminal domain of the current study contained Tryptophan (W), Tyrosine (Y), and Leucine (L). However, domain analysis did not reveal any repetitions of the WY domain, which are characteristic of most RXLR proteins in the C-terminal regions (Anderson *et al.*, 2015). In different effectors, the WY domain is found singly or as divergent tandem repeats (Zhao *et al.*, 2018). Goss *et al.* (2013) have reported that RXLR genes from *P. ramorum* show variation in the copy number of the WY domain. As observed within regions containing WY, the WY domain may represent a platform capable of supporting polymorphism in surface residues, variation in the copy number of repeats, insertions within these repeats, and oligomerisation (Anderson *et al.*, 2015). According to Win *et al.* (2012), the WY domains appear to be a feature which is unique to *Phytophthora* and downy mildew causing phytopathogens, indicating that the WY fold could have played an important role during the evolution of RXLR effectors (Anderson *et al.*, 2015).

Various physicochemical properties of the RXLR protein were assessed using the ProtParam tool. The predicted molecular weight of RXLR protein was 15.52 K Da. Several phytopathogens, including bacteria, fungi, and oomycetes, secrete several low molecular weight protein effectors, which are believed to modulate plant immune responses and enhance pathogenicity (Liu *et al.*, 2018). The instability index estimates the protein's stability- a protein whose instability index is below 40 is estimated to be stable, while the protein is projected to be unstable at a value above 40 (Guruprasad *et al.*, 1990; Gamage *et al.*, 2019). The RXLR effector protein investigated in the current study was stable since it had an instability index of 29.52. As increasing GRAVY scores suggest greater hydrophobicity, the negative GRAVY indices of all proteins tested demonstrated their affinity with

water (Chang and Yang, 2013; Magdeldin *et al.*, 2012). We observed that the RXLR protein was less charged and lower in GRAVY, suggesting that the protein was hydrophilic (Tyler, 2009; Singh *et al.*, 2017; Yang *et al.*, 2020). These findings suggest that the RXLR protein possessed the properties needed to act extra-cellularly.

The secretory protein features were identified using TargetP, SignalP and TMHMM servers, similar to the analysis carried out earlier in *P. sojae*, *P. ramorum*, *P. capsici*, and *P. infestans* (Ye *et al.*, 2015). Three domains: the signal peptide domain, RXLR domain, and effector domain, were predicted by InterProScan. Related domain patterns have been reported for RXLR effectors from oomycetes like *P. infestans*, *P. capsici* and *P. sojae* (Birch *et al.*, 2009; Boutemy *et al.*, 2011; Win *et al.*, 2012). We found the presence of the RXLR-dEER motif in the RXLR effector, which was in line with the previous studies of Jiang *et al.* (2008), Boutemy *et al.* (2011) and Guo *et al.* (2020). A central alpha-helical fold is formed at both the N and C termini of the WY-domain, which is capable of tolerating significant plasticity. Furthermore, it promotes amino acid substitutions in surface residues and oligomerisation as additional alteration mechanisms (Boutemy *et al.*, 2011). By using JPred 4, the secondary structure of the RXLR protein was predicted. The analysis revealed that the protein contained five helical regions, which concur with Ye *et al.* (2015). They reported that short alpha-helices were a typical structural feature of oomycete RXLR effector proteins.

All 3D models were predicted by SPARKS-X and Phyre2 servers. The Ramachandran plot constructed validated that the structure predicted by SPARKS-X was better, with more than 90 per cent residues in the favoured region. After refinement of the models by the ModRefiner server, Model 4 showed a better ProSA score (Z-Score) of -4.02, indicating that the quality of the structure was good (Wiederstein and Sippl, 2007). The refined 3D structure of RXLR protein satisfied all the validation criteria based on the Ramachandran plot analysis (Fig. 3). According to the Ramachandran plot analysis of the predicted structure, 94.0 per cent residues of Φ/Ψ angles are in the most favoured regions, 4.5 per cent residues in the allowed region

and just two residues (1.5%) in the disallowed region. In addition, the structure's overall quality factor was 94.4, which indicates that the structure is of high quality. Generally, high-quality protein structures generate values greater than 50 (Messaoudi *et al.*, 2013). The structural topology revealed that the signal peptide was obtained in a single helical unit and the N-terminal region was a four-helical bundle of abundance as observed in RXLR protein in *P. infestans* (Yaeno *et al.*, 2011; Maqbool *et al.*, 2016).

The present study describes the molecular and structural characterisation of a highly expressed RXLR effector protein from *P. palmivora*, incitant of coconut bud rot disease. To analyse structure-function relationships more precisely, it is necessary to determine the three-dimensional structures of the RXLR protein family from *P. palmivora*. Correlating their structural determinants with their biological activities requires further research.

Acknowledgement

The authors thank the Indian Council of Agricultural Research (ICAR), New Delhi, India, for funding (ICAR-CPCRI Project no. 1000761030).

References

- Ai, G., Yang, K., Ye, W., Tian, Y., Du, Y., Zhu, H., Li, T., Xia, Q., Shen, D., Peng, H. and Jing, M. 2020. Prediction and characterisation of RXLR effectors in *Pythium* species. *Molecular Plant-Microbe Interactions* **33**: 1046-1058.
- Anderson, R.G., Deb, D., Fedkenheuer, K. and McDowell, J.M. 2015. Recent progress in RXLR effector research. *Molecular Plant-Microbe Interactions* **28**: 1063-1072.
- Armstrong, M.R., Whisson, S.C., Pritchard, L., Bos, J.I., Venter, E., Avrova, A.O., Rehmany, A.P., Böhme, U., Brooks, K., Cherevach, I. and Hamlin, N. 2005. An ancestral oomycete locus contains late blight avirulence gene Avr3a, encoding a protein that is recognised in the host cytoplasm. *Proceedings of the National Academy of Sciences USA* **102**: 7766-7771.
- Birch, P.R., Armstrong, M., Bos, J., Boevink, P., Gilroy, E.M., Taylor, R.M., Wawra, S., Pritchard, L., Conti, L., Ewan, R. and Whisson, S.C. 2009. Towards understanding the virulence functions of RXLR effectors of the oomycete plant pathogen *Phytophthora infestans*. *Journal of Experimental Botany* **60**: 1133-1140.
- Birch, P.R., Rehmany, A.P., Pritchard, L., Kamoun, S. and Beynon, J.L. 2006. Trafficking arms: oomycete effectors enter host plant cells. *Trends in Microbiology* **14**: 8-11.
- Boutemy, L.S., King, S.R., Win, J., Hughes, R.K., Clarke, T.A., Blumenschein, T.M., Kamoun, S. and Banfield, M.J. 2011. Structures of *Phytophthora* RXLR effector proteins: A conserved but adaptable fold underpins functional diversity. *Journal of Biological Chemistry* **286**: 35834-35842.
- Chang, K.Y. and Yang, J.R. 2013. Analysis and prediction of highly effective antiviral peptides based on random forests. *PLoS One* **8**: e70166. [https://doi: 10.1371/journal.pone.0070166](https://doi.org/10.1371/journal.pone.0070166).
- Chepsergon, J., Motaung, T.E. and Moleleki, L.N. 2021. "Core" RXLR effectors in phytopathogenic oomycetes: A promising way to breeding for durable resistance in plants? *Virulence* **12**: 1921-1935.
- Drenth, A. and Sendall, B. 2004. Economic impact of *Phytophthora* diseases in Southeast Asia. *Diversity and management of Phytophthora in Southeast Asia*. Drenth, A. and Guest, D. I., Southeast Asia, pp. 10-28.
- Erwin, D.C. and Ribeiro, O.K. 1996. *Phytophthora Diseases Worldwide*. American Phytopathological Society (APS Press).
- Gamage, D.G., Gunaratne, A., Periyannan, G.R. and Russell, T.G. 2019. Applicability of instability index for in vitro protein stability prediction. *Protein and Peptide Letters* **26**: 339-347.
- Gangaraj, K.P. and Rajesh, M.K. 2020. Dataset of dual RNA-sequencing of *Phytophthora palmivora* infecting coconut (*Cocos nucifera* L.). *Data in Brief* **30**: doi: 10.1016/j.dib.2020.105455.
- Gangaraj, K. P., Muralikrishna, K.S., Antony, G., Binod Bihari, S., Hegde, V. and Rajesh, M.K. 2021. A rapid *in vitro* leaf inoculation assay to investigate *Phytophthora palmivora*-coconut interactions. *Journal of Phytopathology* **169**: 316-328.
- Goss, E.M., Press, C.M. and Grünwald, N.J. 2013. Evolution of RXLR-class effectors in the oomycete plant pathogen *Phytophthora ramorum*. *PLoS One* **8**: e79347.
- Guo, Y., Dupont, P.Y., Mesarich, C.H., Yang, B., McDougal, R.L., Panda, P., Dijkwel, P., Studholme, D.J., Sambles, C., Win, J. and Wang, Y. 2020. Functional analysis of RXLR effectors from the New Zealand kauri dieback pathogen *Phytophthora agathidicida*. *Molecular Plant Pathology* **21**: 1131-1148.
- Guruprasad, K., Reddy, B.B. and Pandit, M.W. 1990. Correlation between stability of a protein and its dipeptide composition: a novel approach for predicting in vivo stability of a protein from its primary sequence. *Protein Engineering, Design and Selection* **4**: 155-161.

- Huang, G., Liu, Z., Gu, B., Zhao, H., Jia, J., Fan, G., Meng, Y., Du, Y. and Shan, W. 2019. An RXLR effector secreted by *Phytophthora parasitica* is a virulence factor and triggers cell death in various plants. *Molecular Plant Pathology* **20**: 356-371.
- Hunziker, L., Tarallo, M., Gough, K., Guo, M., Hargreaves, C., Loo, T.S., McDougal, R.L., Mesarich, C.H. and Bradshaw, R.E. 2021. Apoplastic effector candidates of a foliar forest pathogen trigger cell death in host and non-host plants. *Scientific Reports* **11**: 19958. <https://doi.org/10.1038/s41598-021-99415-5>.
- Jiang, R.H., Tripathy, S., Govers, F. and Tyler, B.M. 2008. RXLR effector reservoir in two *Phytophthora* species is dominated by a single rapidly evolving superfamily with more than 700 members. *Proceedings of the National Academy of Sciences USA* **105**: 4874-4879.
- Judelson, H.S. and Blanco F.A. 2005. The spores of *Phytophthora*: weapons of the plant destroyer. *Nature Reviews Microbiology* **3**: 47-58.
- Kamoun, S. 2006. A catalogue of the effector secretome of plant pathogenic oomycetes. *Annual Reviews of Phytopathology* **44**: 41-60.
- Liu, Y., Lan, X., Song, S., Yin, L., Dry, I.B., Qu, J., Xiang, J. and Lu, J. 2018. *In planta* functional analysis and subcellular localisation of the oomycete pathogen *Plasmopara viticola* candidate RXLR effector repertoire. *Frontiers in Plant Science* **9**: 286. <https://doi.org/10.3389/fpls.2018.00286>.
- Magdeldin, S., Yoshida, Y., Li, H., Maeda, Y., Yokoyama, M., Enany, S., Zhang, Y., Xu, B., Fujinaka, H., Yaoita, E. and Sasaki, S. 2012. Murine colon proteome and characterisation of the protein pathways. *Bio Data Mining* **5**: 1-14.
- Maqbool, A., Hughes, R.K., Dagdas, Y.F., Tregidgo, N., Zess, E., Belhaj, K., Round, A., Bozkurt, T.O., Kamoun, S. and Banfield, M.J. 2016. Structural basis of host autophagy-related protein 8 (ATG8) binding by the Irish potato famine pathogen effector protein PexRD54. *Journal of Biological Chemistry* **291**: 20270-20282.
- McHau, G.R.A. and Coffey, M. D. 1994. Isozyme diversity in *Phytophthora palmivora*: Evidence for a southeast Asian centre of origin. *Mycological Research* **98**: 1035-1043.
- Messaoudi, A., Belguith, H. and Hamida, J.B. 2013. Homology modeling and virtual screening approaches to identify potent inhibitors of VEB-1 β -lactamase. *Theoretical Biology and Medical Modelling* **10**: 1-10.
- Petre, B., Contreras, M.P., Bozkurt, T.O., Schattat, M.H., Sklenar, J., Schornack, S., Abd-El-Haliem, A., Castells-Graells, R., Lozano-Duran, R., Dagdas, Y. and Menke, F. 2020. Host-interactor screens of *Phytophthora infestans* RXLR proteins reveal vesicle trafficking as a major effector-targeted process. *The Plant Cell* **33**:1447-1471.
- Rehmany, A.P., Gordon, A., Rose, L.E., Allen, R.L., Armstrong, M.R., Whisson, S.C., Kamoun, S., Tyler, B.M., Birch, P.R. and Beynon, J.L. 2005. Differential recognition of highly divergent downy mildew avirulence gene alleles by *RPP1* resistance genes from two *Arabidopsis* lines. *The Plant Cell* **17**(6): 1839-1850.
- Rey, T., Chatterjee, A., Buttay, M., Toulotte, J. and Schornack, S. 2015. *Medicago truncatula* symbiosis mutants affected in the interaction with a biotrophic root pathogen. *New Phytologist* **206**: 497-500.
- Riolo, M., Aloi, F., La Spada, F., Sciandrello, S., Moricca, S., Santilli, E., Pane, A. and Cacciola, S.O. 2020. Diversity of *Phytophthora* communities across different types of Mediterranean vegetation in a nature reserve area. *Forests* **11**: 853.
- Rose, J.K., Ham, K.S., Darvill, A.G. and Albersheim, P. 2002. Molecular cloning and characterisation of glucanase inhibitor proteins: co-evolution of a counter defense mechanism by plant pathogens. *The Plant Cell* **14**: 1329-1345.
- Scanu, B., Jung, T., Masigol, H., Linaldeddu, B.T., Jung, M.H., Brandano, A., Mostowfizadeh-Ghalamfarsa, R., Janoušek, J., Riolo, M. and Cacciola, S.O. 2021. *Phytophthora heterospora* sp. nov., a new pseudoconidia-producing sister species of *P. palmivora*. *Journal of Fungi* **7**: 870. <https://doi.org/10.3390/jof7100870>.
- Schornack, S., Huitema, E., Cano, L.M., Bozkurt, T.O., Oliva, R., van Damme, M., Schwizer, S., Raffaele, S., Chaparro Garcia, A., Farrer, R., Segretin, M.E., Bos, J., Haas, B.J., Zody, M.C., Nusbaum, C., Win, J., Thines, M. and Kamoun, S. 2009. Ten things to know about oomycete effectors. *Molecular Plant Pathology* **10**: 795- 803.
- Scott, P., Burgess, T. and Hardy, GESJ 2013. Globalisation and *Phytophthora*. *Phytophthora: A Global Perspective*. CABI Plant Protection Series, Oxfordshire, UK. pp. 226-232.
- Shan, W., Cao, M., Leung, D. and Tyler, B.M. 2004. The *Avr1b* locus of *Phytophthora sojae* encodes an elicitor and a regulator required for avirulence on soybean plants carrying resistance gene Rps 1b. *Molecular Plant-Microbe Interactions* **17**: 394-403.
- Singh, Y., Patil, V.U., Dhasmana, A., Chakraborty, S.K., Shukla, P.K. and Rawat, S., 2017. *In silico* study of RXLR effectors of *Phytophthora infestans* HP-10-31, A2 mating type potato late blight pathogen. *International Journal of Advanced Biotechnology and Research* **8**: 398.
- Tian, M., Benedetti, B. and Kamoun, S. 2005. A second Kazal-like protease inhibitor from *Phytophthora infestans* inhibits and interacts with the apoplastic pathogenesis-related protease P69B of tomato. *Plant Physiology* **138**: 1785-1793.

- Tian, M., Huitema, E., Da Cunha, L., Torto-Alalibo, T. and Kamoun, S. 2004. A Kazal-like extracellular serine protease inhibitor from *Phytophthora infestans* targets the tomato pathogenesis-related protease P69B. *Journal of Biological Chemistry* **279**: 26370-26377.
- Tyler, B.M., 2009. Entering and breaking: virulence effector proteins of oomycete plant pathogens. *Cellular Microbiology* **11**: 13-20.
- van Poppel, P.M., Guo, J., van de Vondervoort, P.J., Jung, M.W., Birch, P.R., Whisson, S.C. and Govers, F. 2008. The *Phytophthora infestans* avirulence gene *Avr4* encodes an RXLR-dEER effector. *Molecular Plant-Microbe Interactions* **21**: 1460-1470.
- Wang, S., McLellan, H., Bukharova, T., He, Q., Murphy, F., Shi, J., Sun, S., van Weymers, P., Ren, Y., Thilliez, G. and Wang, H. 2019. *Phytophthora infestans* RXLR effectors act in concert at diverse subcellular locations to enhance host colonisation. *Journal of Experimental Botany* **70**: 343-356.
- Whisson, S.C., Boevink, P.C., Moleleki, L., Avrova, A.O., Morales, J.G., Gilroy, E.M., Armstrong, M.R., Grouffaud, S., Van West, P., Chapman, S. and Hein, I. 2007. A translocation signal for delivery of oomycete effector proteins into host plant cells. *Nature* **450**: 115-118.
- Wiederstein, M. and Sippl, M.J. 2007. ProSA-web: interactive web service for the recognition of errors in three-dimensional structures of proteins. *Nucleic Acids Research* **35**: W407-W410.
- Win, J., Krasileva, K.V., Kamoun, S., Shirasu, K., Staskawicz, B.J. and Banfield, M.J. 2012. Sequence divergent RXLR effectors share a structural fold conserved across plant pathogenic oomycete species. *PLoS Pathogens* **8**: e1002400. <https://doi.org/10.1371/journal.ppat.1002400>.
- Yaeno, T., Li, H., Chaparro-Garcia, A., Schornack, S., Koshiba, S., Watanabe, S., Kigawa, T., Kamoun, S. and Shirasu, K. 2011. Phosphatidylinositol monophosphate-binding interface in the oomycete RXLR effector AVR3a is required for its stability in host cells to modulate plant immunity. *Proceedings of the National Academy of Sciences USA* **108**: 14682-14687.
- Yang, L.N., Liu, H., Duan, G.H., Huang, Y.M., Liu, S., Fang, Z.G., Wu, E.J., Shang, L. and Zhan, J. 2020. The *Phytophthora infestans* AVR2 effector escapes R2 recognition through effector disordering. *Molecular Plant-Microbe Interactions* **33**: 921-931.
- Ye, W., Wang, Y. and Wang, Y. 2015. Bioinformatics analysis reveals abundant short alpha-helices as a common structural feature of oomycete RXLR effector proteins. *PLoS One* **10**: e0135240. [https://doi: 10.1371/journal.pone.0135240](https://doi.org/10.1371/journal.pone.0135240).
- Yoshida, K., Schuenemann, V.J., Cano, L.M., Pais, M., Mishra, B., Sharma, R., Lanz, C., Martin, F.N., Kamoun, S., Krause, J. and Thines, M. 2013. The rise and fall of the *Phytophthora infestans* lineage that triggered the Irish potato famine. *Elife* **2**: e00731.
- Zhao, L., Zhang, X., Zhang, X., Song, W., Li, X., Feng, R., Yang, C., Huang, Z. and Zhu, C., 2018. Crystal structure of the RXLR effector PcrXLR12 from *Phytophthora capsici*. *Biochemical and Biophysical Research Communications* **503**: 1830-1835.
- Zuluaga, A.P., Vega-Arreguín, J.C., Fei, Z., Matas, A.J., Patev, S., Fry, W.E. and Rose, J.K. 2016. Analysis of the tomato leaf transcriptome during successive hemibiotrophic stages of a compatible interaction with the oomycete pathogen *Phytophthora infestans*. *Molecular Plant Pathology* **17**: 42-54.